

THE ROLE OF ENVIRONMENT IN THE MASS–METALLICITY RELATION

MICHAEL C. COOPER^{1,2}, CHRISTY A. TREMONTI^{1,3}, JEFFREY A. NEWMAN⁴, ANN I. ZABLUDOFF¹

Draft version November 26, 2018

ABSTRACT

Using a sample of 57,377 star-forming galaxies drawn from the Sloan Digital Sky Survey, we study the relationship between gas-phase oxygen abundance and environment in the local Universe. We find that there is a strong relationship between metallicity and environment such that more metal-rich galaxies favor regions of higher overdensity. Furthermore, this metallicity–density relation is comparable in strength to the color–density relation along the blue cloud. After removing the mean dependence of environment on color and luminosity, we find a significant residual trend between metallicity and environment that is largely driven by galaxies in high-density regions, such as groups and clusters. We discuss the potential source of this relationship between metallicity and local galaxy density in the context of feedback models, with special attention paid to quantifying the impact of environment on the scatter in the mass–metallicity relation. We find that environment is a non-negligible source of scatter in this fundamental relation, with $\gtrsim 15\%$ of the measured scatter correlated with environment.

Subject headings: galaxies:evolution, galaxies:statistics, galaxies: abundances, galaxies:fundamental parameters, large-scale structure of universe

1. INTRODUCTION

Gas-phase metallicity is one of the most fundamental characteristics of a galaxy, affecting the evolution of its stellar population and the composition of its interstellar medium (ISM). Moreover, metallicity indirectly traces a galaxy’s star-formation history and reflects the balance of several important physical processes: the release of metals into the interstellar medium via supernovae and stellar winds, the ejection of gas via galactic outflows, and the accretion of gas onto the galaxy from the surrounding environs. Understanding how metallicity evolves, especially in relation to other fundamental galaxy properties, is essential in isolating the physical mechanisms that drive star formation and, more generally, galaxy evolution.

As first observed by Lequeux et al. (1979), metallicity is strongly correlated with galaxy stellar mass, such that more massive galaxies are more metal-rich in composition. Due to the relative ease of measuring luminosities versus stellar masses, many subsequent studies extended this early work to larger samples of galaxies by studying the correlation between luminosity and metallicity (e.g., Skillman et al. 1989; Brodie & Huchra 1991; Zaritsky et al. 1994; Garnett 2002; Kobulnicky et al. 2003; Lamareille et al. 2004). Using large data sets from surveys such as the Sloan Digital Sky Survey (SDSS, York et al. 2000), more recent analyses have brought measurements of the luminosity– and mass–metallicity relations on par with each other, measuring relations that span more than ten magnitudes in optical luminosity and six orders of mag-

nitude in stellar mass, ranging from dwarf galaxies up to the most massive star-forming systems (e.g., Pilyugin & Ferrini 2000; Lee et al. 2003; Tremonti et al. 2004; Shapley et al. 2005; Erb et al. 2006; Lee et al. 2006).

Both the luminosity–metallicity and mass–metallicity relations show significant scatter, with only half the observed spread in the metallicity distribution at fixed stellar mass being due to observational error and an even greater ($\sim 50\%$ greater) scatter measured for the luminosity–metallicity relation (Tremonti et al. 2004). Various studies have pointed to physical sources of the scatter in these fundamental relations. For example, studying a sample of UV-selected galaxies at $z < 0.4$, Contini et al. (2002) find that these systems are offset from the luminosity–metallicity relation due to a recent starburst that has enriched their ISM and decreased their mass-to-light ratios, moving them off of the median trend. As illustrated by Tremonti et al. (2004), however, these results suggest that the relationship between metallicity and stellar mass (and not luminosity) is more fundamental; even when accounting for variations in mass-to-light ratio due to dust attenuation and observing at redder wavelengths so as to minimize the impact of newly formed stars on the measured luminosity, the scatter in the luminosity–metallicity relation is still greater than that observed between stellar mass and metallicity.

By analyzing the correlations between the scatter in the mass–metallicity relation and other galaxy properties (e.g., rest-frame color, inclination, photometric concentration, etc.), Tremonti et al. (2004) point to a potential connection with stellar surface mass density, μ_* , such that galaxies with higher surface densities are more metal-rich relative to galaxies of similar stellar mass (see also Ellison et al. 2008a). This trend is potentially explained by a scenario where galaxies with higher surface densities have converted more of their gas reservoirs into stars and thereby elevated their metallicity. In conflict with this picture, however, Tremonti et al. (2004) find

¹ Steward Observatory, University of Arizona, 933 N. Cherry Avenue, Tucson, AZ 85721 USA; cooper@as.arizona.edu, tremonti@as.arizona.edu, azabludoff@as.arizona.edu

² Spitzer Fellow

³ Hubble Fellow

⁴ Department of Physics and Astronomy, University of Pittsburgh, 401-C Allen Hall, 3941 O’Hara Street, Pittsburgh, PA 15260 USA; janewman@pitt.edu

no significant correlation between scatter in the mass–metallicity relation and morphology (as traced by the concentration).

Local galaxy density (i.e., the local “environment”) could act as an alternate source of the scatter in the mass–metallicity relation. Supernovae are predicted to enrich the intergalactic medium (IGM) over roughly Mpc scales (e.g., Adelberger et al. 2005), which would impact the metallicity of nearby galaxies in high–density environments. Similarly, in clusters of galaxies, intracluster supernovae may inject a significant quantity of metals into the intracluster gas (Domainko et al. 2004), which is subsequently accreted onto cluster members, thereby raising their metallicity.

Galaxies in high–density regions should collapse and form stars earlier than their counterparts in low–density environs; studies of the color–density relation show that galaxies with older stellar populations favor higher–density environments at $z \sim 0$ (e.g., Balogh et al. 2004a,b; Blanton et al. 2005a) and at $z \sim 1$ (e.g., Cooper et al. 2006; Smith et al. 2005). Thus, galaxies might be expected to become more metal–rich sooner in high–density regions.

Direct evidence for the potential role of environment in shaping the metallicity of a galaxy is found in observational work by Kewley et al. (2006), which shows that galaxy interactions, common in galaxy pairs and groups (Cavaliere et al. 1992), may lead to inflows that drag metal–poor gas to the galaxy center, decreasing the gas–phase metallicity in such systems (see also Ellison et al. 2008b). The analysis of Kewley et al. (2006), however, probes a limited range of extreme environments (focusing on pairs at close separations), which provides a vastly incomplete view of the role of environment. Similarly, analysis of 41 metal–rich, low–mass galaxies by Peeples et al. (2008), finds that such outliers on the mass–metallicity relation tend to be isolated and undisturbed systems (i.e., reside in low–density environments). Though, this work is clearly limited by its small sample size and the restricted mass range probed.

In this paper, we utilize data from the Sloan Digital Sky Survey to study the relationship between metallicity and environment among the nearby, star–forming galaxy population. Specifically, we inspect the correlation between metallicity and environment in comparison to well–established correlations between environment and properties such as rest–frame color. In addition, we examine the potential impact of environment on the scatter in the mass–metallicity relation. In §2, we outline the data set used in this analysis. In §3, §4, and §5, we present our results on the relationship between metallicity and environment at $z \sim 0.1$. We then endeavor to quantify the role of environment in driving the scatter in the mass–metallicity relation in §6. In §7 and §8, the results of this analysis are then discussed and summarized. Unless otherwise noted, all work in this paper employs a flat, $\Omega_\Lambda = 0.7$, $\Omega_m = 0.3$, $h = 1$ cosmology.

2. DATA SAMPLE

To study the relationship between local galaxy environment and various galaxy properties, including metallicity, we utilize data drawn from the SDSS public data release 4 (DR4, Adelman-McCarthy et al. 2006), as contained in the NYU Value–Added Galaxy Catalog (NYU–

VAGC, Blanton et al. 2005b). We restrict our analysis to the redshift regime $0.05 < z < 0.15$ in an effort to probe a broad range in galaxy luminosity, with large sample size, while minimizing aperture effects related to the finite size (3”) of the SDSS fibers. In addition, we limit our sample to SDSS fiber plates for which the redshift success rate for targets in the main spectroscopic survey is 80% or greater.

2.1. Measurements of Local Galaxy Environments

We estimate the local galaxy overdensity, or “environment”, in the SDSS using measurements of the projected 3rd–nearest–neighbor surface density (Σ_3) about each galaxy, where the surface density depends on the projected distance to the 3rd–nearest neighbor, $D_{p,3}$, as $\Sigma_3 = 3/(\pi D_{p,3}^2)$. In computing Σ_3 , a velocity window of ± 1000 km/s is employed to exclude foreground and background galaxies along the line–of–sight. Tests by Cooper et al. (2005) found this environment estimator to be a robust indicator of local galaxy density within deep surveys.

To correct for the redshift dependence of the SDSS sampling rate, each surface density value is divided by the median Σ_3 of galaxies at that redshift within a window of $\Delta z = 0.02$; this converts the Σ_3 values into measures of overdensity relative to the median density (given by the notation $1 + \delta_3$ here) and effectively accounts for redshift variations in the selection rate (Cooper et al. 2005). Finally, to minimize the effects of edges and holes in the SDSS survey geometry, we exclude all galaxies within $1 h^{-1}$ Mpc (comoving) of a survey boundary. For further details regarding the computation of galaxy environments in the SDSS, we direct the reader to Cooper et al. (2006) and Cooper et al. (2008).

2.2. Measurements of Rest–frame Color, Absolute Magnitude, and Stellar Mass

We compute rest–frame $g - r$ colors, absolute r –band magnitudes (M_r), and stellar masses from the apparent, petrosian *ugriz* magnitudes in the SDSS DR4, using the *kcorrect* K–correction code (version v4_1_2) of Blanton & Roweis (2007, see also Blanton et al. 2003a). The template SEDs employed by *kcorrect* are based on those of Bruzual & Charlot (2003). To estimate stellar masses, the best–fit SED given the observed *ugriz* photometry and spectroscopic redshift is used to directly compute the stellar mass–to–light ratio (M_*/L), assuming a Chabrier (2003) initial mass function. We have also employed the stellar mass estimates of Kauffmann et al. (2003a), which do not rely on fitting SEDs to the SDSS photometry; instead they have been derived by fitting to stellar absorption–line indices, measured from the observed SDSS spectra, while also attempting to correct for attenuation due to dust. Using these alternate stellar mass values produces no significant changes in the results of our analyses. Finally, all magnitudes within this paper are given in the AB system (Oke & Gunn 1983).

2.3. Measurements of Spectral Properties: Metallicity and Star–Formation Rate

To study the metallicities of the SDSS galaxies, we utilize oxygen abundances, $12 + \log_{10}(\text{O}/\text{H})$, from

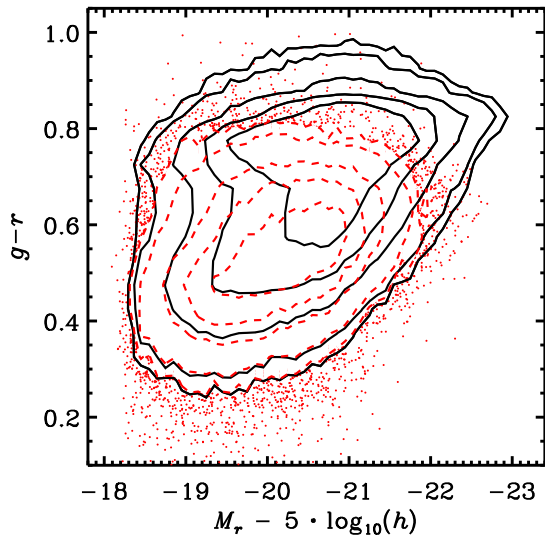


FIG. 1.— The color–magnitude distribution for all 246,242 galaxies within $0.05 < z < 0.15$ in the SDSS NYU–VAGC DR4 catalog (*black solid lines*) and for the 57,377 star–forming galaxies with accurate environment and metallicity measurements in the redshift range $0.05 < z < 0.15$ (*red points and dashed lines*). The dominant impact of the cuts made in selecting our star–forming sample is the exclusion of quiescent galaxies and AGN, which preferentially reside at the red end of the blue cloud or on the red sequence.

Tremonti et al. (2004), which have been derived by statistically comparing the fits of nebular emission lines in the SDSS spectra to the models of Charlot & Longhetti (2001). The sample is limited to only those sources with $H\beta$, $H\alpha$, and $[N\ II]\ \lambda 6584$ all detected at a 5σ level. Furthermore, we constrain our analysis to the star–forming galaxy sample, excluding those objects hosting an active galactic nucleus (AGN) according to the conservative line–diagnostic criteria of Kauffmann et al. (2003b). By also requiring accurate environment measures, as described above, we arrive at a final star–forming galaxy sample including 57,377 sources at $0.05 < z < 0.15$. A distribution of the sample in color–magnitude space is shown in Figure 1. By excluding quiescent galaxies and active galactic nuclei (AGN), the star–forming sample is biased against galaxies residing on the red end of the blue cloud or the red sequence. In Figure 2, we also show the distribution of environment measures for the star–forming sample relative to that for the full SDSS sample. While the star–forming galaxies are biased towards lower overdensities (consistent with a sample dominated by blue galaxies), the sample still spans a full range of environments, from voids to clusters.

To probe the ongoing star–formation activity in this sample, we employ the aperture–corrected star–formation rates (SFR) of Brinchmann et al. (2004), which are estimated by fitting models to the nebular emission features in the SDSS spectra. For the star–forming galaxy population, these SFRs show excellent agreement with UV–based star–formation rate estimates (Salim et al. 2007). Note that the SFR values of Brinchmann et al. (2004) are estimated using $h = 0.7$ rather than $h = 1$.

3. THE DEPENDENCE OF MEAN ENVIRONMENT ON METALLICITY

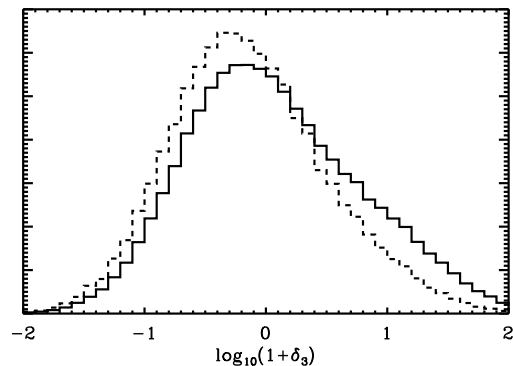


FIG. 2.— The distribution of the logarithm of the local overdensities, $\log_{10}(1 + \delta_3)$, for all 232,882 SDSS galaxies within $0.05 < z < 0.15$ and with accurate environment measurements (*solid line*) and for the 57,377 star–forming galaxies with accurate environment and metallicity measurements (*dashed line*). Here, we scale the two histograms so that their integrals are equal. The star–forming galaxies are biased towards lower overdensities, though the sample still spans the full range of environments probed by the SDSS.

A wide variety of galaxy properties at low and intermediate redshift have been shown to correlate with environment. For instance, at $z < 1$, blue, star–forming galaxies are found to reside in regions of lower galaxy density in comparison to red and dead systems (e.g., Balogh et al. 1998; Kauffmann et al. 2004; Cooper et al. 2006; Cucciati et al. 2006; Capak et al. 2007). Moving beyond direct studies of the color–density or morphology–density relations, Blanton et al. (2005a) analyzed the relationship between environment and the luminosities, surface brightnesses, rest–frame colors, and structural characteristics (Sérsic indices) of nearby galaxies in the SDSS sample. Among this set of galaxy properties, they found that color and luminosity are the pair that prove to be most predictive of the local environment. That is, rest–frame color and luminosity are the two characteristics most closely related to the galaxy density, as measured on small ($\sim 1\ h^{-1}\ \text{Mpc}$) scales. Furthermore, at fixed color and luminosity, they found no significant trend between local galaxy density and surface brightness or Sérsic index among the star–forming population — although, for the full SDSS sample, there is some residual correlation observed at high luminosities, likely driven by rare, very luminous, red systems in dense environments such as brightest cluster galaxies (Blanton et al. 2005a).

Like surface brightness and Sérsic index, metallicity is strongly correlated with color and luminosity, such that brighter and redder sources on the blue cloud tend to have higher metal abundances. This trend is clearly evident in the top panel of Figure 3, where we show the mean gas–phase oxygen abundance, $12 + \log_{10}(O/H)$, as a function of rest–frame color and absolute magnitude for the SDSS star–forming sample. Not surprisingly, when we examine the relationship between metallicity and environment, we find a strong trend that includes contributions from the correlations between (a) metallicity, color, and luminosity and (b) color, luminosity, and environment. As shown in the bottom portion of Figure 3, the typical environment increases in

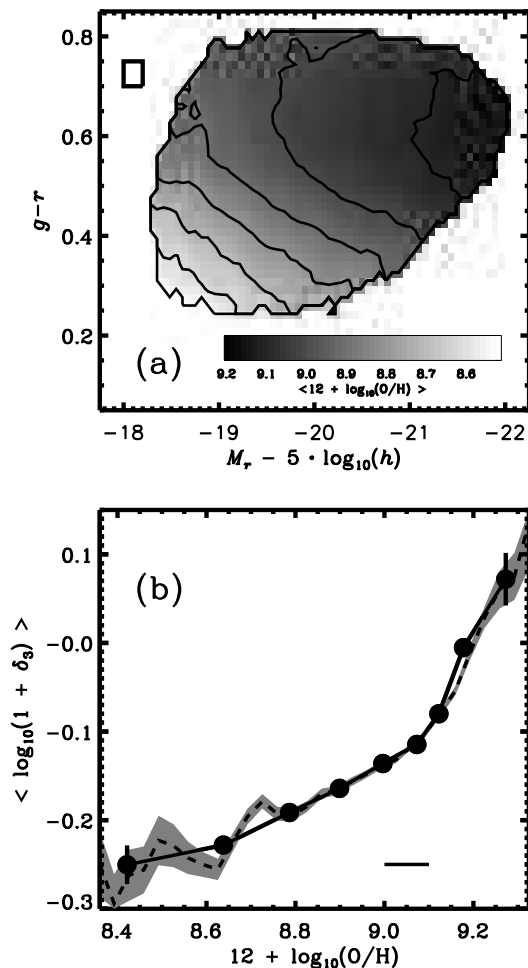


FIG. 3.— (Top) We plot the mean gas-phase metallicity, $12 + \log_{10}(\text{O}/\text{H})$, as a function of rest-frame color and absolute magnitude, computed in a sliding box of width $\Delta M_r = 0.2$ and height $\Delta(g-r) = 0.05$, as shown in the upper left corner. The mean metallicity depends on both color and luminosity, with more luminous and redder galaxies tending to have greater metal content. (Bottom) We plot the mean galaxy overdensity as a function of gas-phase metallicity for the star-forming population. The dashed black line and grey shaded region show the mean and 1σ uncertainty in the mean overdensity computed in a sliding box of width $\Delta(12 + \log_{10}(\text{O}/\text{H})) = 0.1$. The points and corresponding error bars give the mean and 1σ error in the mean in discrete bins of metallicity. We compute overdensities using the full SDSS galaxy sample (i.e., not just the star-forming population), thus the mean values plotted here are generally less than zero (in the logarithm), as expected from the color-density relation.

overdensity for galaxies with higher metallicities.⁵ This metallicity-environment relation agrees with the well-established color-density relation along the blue cloud (Hogg et al. 2003; Blanton et al. 2005a), where the mean galaxy density increases with color.

⁵ The local environment is thought to influence galaxy properties, such that galaxy properties are typically studied as a function of environment. In Figure 3b, however, we plot the dependence of mean environment on metallicity and not vice versa for one significant reason: measurements of environment are significantly more uncertain than measures of metallicity. Thus, binning galaxies according to local overdensity would yield significant correlation between neighboring environment bins, which would consequently smear out the underlying correlation between metallicity and local galaxy overdensity.

While the trend evident in Figure 3b may not be surprising, the *strength* of this environment-metallicity relation is very striking when compared to that seen between environment and color, luminosity, stellar mass, or star-formation rate. As shown in Figure 3b and Figure 4, the metallicity-density relation is roughly comparable in strength to the color-density relation amongst the star-forming population. In addition, the dependence of mean overdensity on luminosity, stellar mass, and SFR are all weaker than that observed with metallicity. Along the blue cloud, there is clearly a strong relationship between gas-phase oxygen abundance and the local galaxy environment.

4. REMOVING THE MEAN COLOR-LUMINOSITY-ENVIRONMENT RELATION

Given the relationships between metallicity, color, and luminosity, it would be reasonable to expect that the strong relationship between local galaxy density and metallicity is entirely contained in the color-luminosity-environment relation (within the precision of our measurements), such that there is no residual trend between metallicity and environment at fixed color and luminosity — similar to the findings of Blanton et al. (2005a) for surface brightness and Sérsic index. To probe the dependence of environment on metallicity at fixed color and luminosity, we fit and remove (subtract) the dependence of mean environment on rest-frame color and absolute magnitude. Figure 5a shows the mean overdensity as a function of rest-frame $g-r$ color and r -band absolute magnitude, or $\langle \log_{10}(1 + \delta_3)[g-r, M_r] \rangle$, for the SDSS star-forming sample. There is a clear color-density trend, where the mean overdensity increases with color along the blue cloud. To remove this relationship of environment to color and luminosity, we subtract the mean overdensity at the color and luminosity of each galaxy from the measured overdensity:

$$\Delta_3 = \log_{10}(1 + \delta_3) - \langle \log_{10}(1 + \delta_3)[g-r, M_r] \rangle, \quad (1)$$

where the distribution of mean environment with color and absolute magnitude, $\langle \log_{10}(1 + \delta_3)[g-r, M_r] \rangle$ (see Fig. 5a), is median smoothed on $\Delta(g-r) = 0.15$ and $\Delta M_r = 0.6$ scales prior to subtraction.

An alternate method of effectively removing the color-luminosity-environment relation from our analysis would be to study the metallicity-environment relation in bins of rest-frame color and absolute magnitude (or in bins of stellar mass). This approach, however, can be far less sensitive, since dividing the sample into such restricted subsets reduces the signal-to-noise ratio of any trend that occurs across the entire color-magnitude distribution (i.e., spans the blue cloud). In §7.3, we return to this point in comparison to other recent, related analyses.

The “residual” environment, Δ_3 , quantifies the overdensity about a galaxy relative to galaxies of similar color and luminosity, where values of Δ_3 greater than zero correspond to galaxies in environments more overdense than the typical galaxy with like star-formation history (that is, like $g-r$ and M_r). Figure 5b shows the dependence of mean Δ_3 on color and luminosity; no significant color or luminosity dependence is evident. Furthermore, Figure 5c displays the distribution of $\langle \Delta_3 \rangle$ values from Fig. 5b, illustrating that deviations from $\langle \Delta_3 \rangle = 0$ are small.

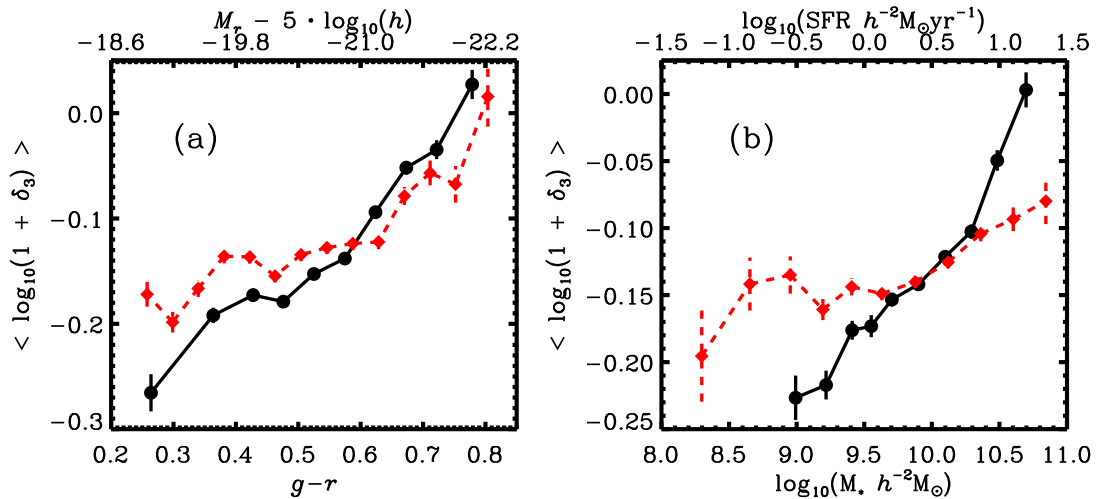


FIG. 4.— (*Left*) For the star-forming population, we plot the dependence of mean overdensity, $\log_{10}(1 + \delta_3)$, on rest-frame color and absolute magnitude, as given by the black circles plus solid line and red diamonds plus dashed line, respectively. (*Right*) Similar to the plot on the left, but for stellar mass, M_* , (black circles and solid line) and star-formation rate (red diamonds and dashed line). Within the star-forming sample, the metallicity–environment trend is as strong as the color–density relation, which is the strongest of the relations plotted here.

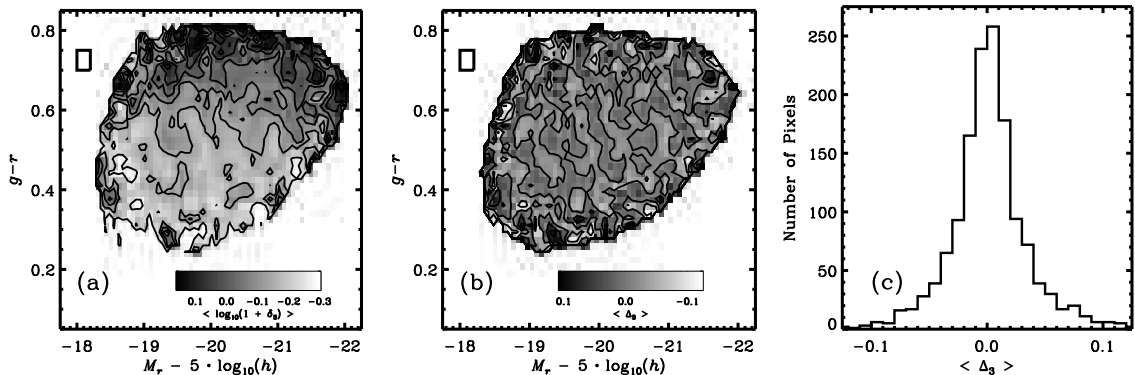


FIG. 5.— (*Left*) For the star-forming sample, we show the mean galaxy overdensity, $\log_{10}(1 + \delta_3)$, as a function of rest-frame galaxy color, $g - r$, and absolute magnitude, M_r , computed in a sliding box of width $\Delta M_r = 0.2$ and height $\Delta(g - r) = 0.05$. The size and shape of the box are illustrated in the upper left corner of the plot. (*Middle*) The mean residual environment, Δ_3 , as a function of color and magnitude, computed in the same sliding box. (*Right*) We plot the distribution of mean residual environment for all regions where the sliding box contains 20 or more galaxies.)

While the Δ_3 statistic effectively removes the mean color–density and luminosity–density relations from the data set, this measure of the residual environment is only a small perturbation to the “absolute” overdensity, $\log_{10}(1 + \delta_3)$. As shown in Figure 6, the Δ_3 value for each galaxy in our sample is still strongly correlated with the corresponding $\log_{10}(1 + \delta_3)$ measurement. This close correlation is, at least in part, due to the large uncertainty in individual overdensity, $\log_{10}(1 + \delta_3)$, measures. The bias towards $\Delta_3 > \log_{10}(1 + \delta_3)$ is a product of the color–density relation and the inclusion of red-sequence galaxies in the measurement of galaxy overdensities (see §2.1).

5. THE RESIDUAL DEPENDENCE OF ENVIRONMENT ON METALLICITY

By studying the dependence of residual environment, Δ_3 , on various galaxy properties, we can determine whether there is any excess trend with environment beyond that contained in the color–luminosity–environment relation. As a sanity check, in Figure 7a

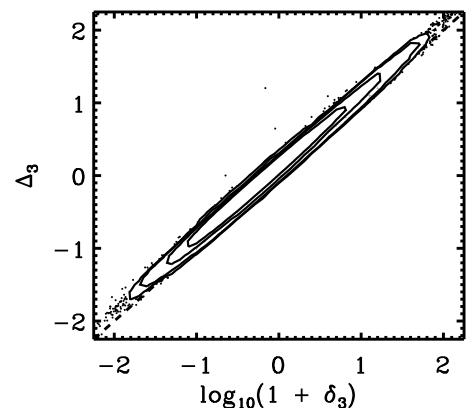


FIG. 6.— For the 57,377 galaxies in the star-forming population, we plot the relationship between the “residual” environment, Δ_3 , and the “absolute” environment, $\log_{10}(1 + \delta_3)$. For a definition of the Δ_3 statistic, refer to Equation 1.

we examine the dependence of mean Δ_3 on color or absolute magnitude, and confirm that there is no trend with these properties, as expected. We likewise test for any dependence of residual environment on stellar mass or star-formation rate (see Figure 7b).

We find no significant trend of Δ_3 with color, luminosity, stellar mass, or SFR. This result is clearly to be expected for color and luminosity, by construction. Given the relatively tight relationship between the combination of $g-r$ and M_r with M_* (e.g., Kauffmann et al. 2003a; Cooper et al. 2007), it is also not surprising to find no residual trend with stellar mass, as an additional test. When using the stellar mass values of Kauffmann et al. (2003a), which were derived from fits to stellar absorption features in the SDSS spectra rather than computed directly from the SDSS photometry (see §2.2), we find a similar lack of any trend. For star-formation rate, which exhibits a weaker correlation with absolute environment, $\log_{10}(1+\delta_3)$, we find no evidence for a relationship with residual environment, Δ_3 , much like the lack of secondary environment-dependencies on surface brightness or Sérsic index found by Blanton et al. (2005a).

Turning our attention towards metallicity, we examine the dependence of mean residual environment, Δ_3 , on gas-phase oxygen abundance; as shown in Figure 8, there is a striking trend such that more metal-rich galaxies typically reside in more overdense environments relative to galaxies of like color and luminosity (i.e., of like stellar mass). While the residual environment statistic, Δ_3 , has no relationship with color, luminosity, stellar mass, or SFR, it is strongly related to metallicity. In particular, this trend seems to be most significant among the most metal-rich galaxies ($12 + \log_{10}(\text{O}/\text{H}) > 9.1$).

Given that the residual environment closely traces the absolute overdensity measurement (see Fig. 6), it is interesting to examine this residual metallicity-environment relation from the opposite perspective. Figure 9 shows the dependence of mean gas-phase oxygen abundance on the residual environment within the SDSS star-forming sample. While studying mean relations from this perspective is physically intuitive, binning galaxies according to environment (residual or absolute) introduces significant correlation between neighboring environment bins, due to the significant uncertainties in measuring local galaxy densities ($\sigma_{\log(1+\delta_3)} \sim 0.5$ versus $\sigma_{12+\log(\text{O}/\text{H})} \sim 0.1$), which can therefore weaken or erase any underlying trends. Despite this smearing effect, we still find a strong trend, where the mean metallicity increases dramatically in higher density regions ($\Delta_3 \gtrsim 1$); this suggests that the residual metallicity-environment relation is dominated by phenomena occurring in overdense regions (such as groups and clusters), rather than underdense environments.

6. SCATTER IN THE MASS-METALLICITY RELATION

The excess correlation between metallicity and environment, beyond that contained in the color-luminosity-environment relation (or stellar mass-environment relation), strongly suggests that the shape or normalization of the mass-metallicity relation must depend on local galaxy environment. This suggestion is confirmed in Figure 10, where we show fits to the mass-metallicity relation, computed using galaxies in the extreme quintiles of the environment distribution. Over the entire range

of stellar masses probed by the SDSS sample, the mass-metallicity relation is biased towards higher metallicities in higher-density regions.

While Figure 10 clearly illustrates the environment dependence of the mass-metallicity relation, showing an offset towards higher metallicity in higher-density regions, it does not *quantify* the level to which environment contributes to the scatter in this fundamental relationship. To this end, we examine the correlation between environment and the residual metallicity, $\Delta_{(\text{O}/\text{H})} = 12 + \log_{10}(\text{O}/\text{H}) - f(M_*)$, measured relative to the median mass-metallicity relation, $f(M_*)$, as determined by the full star-forming sample.

As shown in Figure 11, the average residual metallicity exhibits a clear dependence on environment, such that galaxies in overdense regions are biased towards higher metallicities than galaxies of like stellar mass. This result is effectively a rephrasing of the trend shown in Fig. 9 and Fig. 10, except that in this form we are able to subtract the average offset in the mass-metallicity relation due to environment, yielding a quantity

$$\epsilon = 12 + \log_{10}(\text{O}/\text{H}) - \langle \Delta_{(\text{O}/\text{H})}[\Delta_3] \rangle, \quad (2)$$

which gives the metallicity corrected for the observed environment dependence.

Subtracting (in quadrature) the measured scatter in the mass- ϵ relation from the scatter in the mass-metallicity relation, we find that environment is correlated with $\gtrsim 15\%$ of the observed scatter in the mass-metallicity relation. This environment-dependence is evident, with comparable strength, at all stellar masses. As discussed in §4 and §5, the relatively large uncertainties in the environment measurements can smear out the underlying correlation between metallicity and environment, thereby weakening the measured contribution of environment to the scatter in the mass-metallicity relation. Thus, local environment is correlated with *at least* 15% of the observed scatter, which represents a non-negligible contribution to the total intrinsic scatter.

While we find a significant offset in the normalization of the mass-metallicity relation in different environments, we do not detect any environment-dependent variation in the intrinsic scatter. As shown in Figure 12, the measured root-mean-square (RMS) scatter in the mass-metallicity relation is independent of environment, at a constant level of roughly $\sigma_{\text{O}/\text{H}} \sim 0.1$. This suggests that whatever is dominating the intrinsic scatter in the mass-metallicity relation is independent of local galaxy overdensity.

7. DISCUSSION

7.1. Potential Selection Effects

While we utilize the relatively conservative line-diagnostic criteria of Kauffmann et al. (2003b) for excluding AGN from our sample, any significant amount of contamination from AGN emission in the integrated galaxy spectra could potentially impact the oxygen abundance measurements, biasing them towards high (or low) metallicity. If AGN are strongly correlated with a given environment (e.g., if they are preferentially found in high-density regions), then the metallicity-density relation could be (at some level) a product of this underlying AGN-environment correlation. Of particular inter-

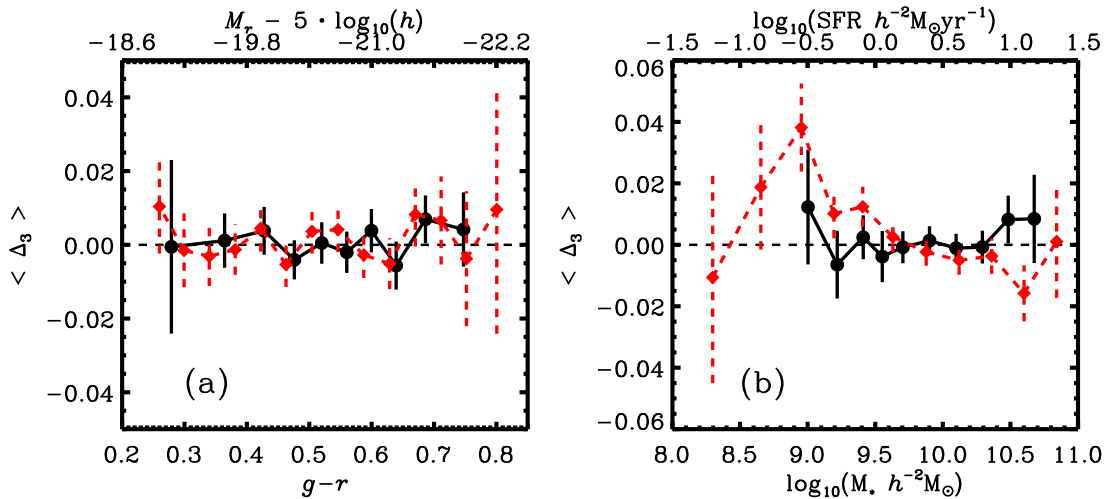


FIG. 7.— (Left) The dependence of mean residual environment, Δ_3 , on rest-frame color and absolute magnitude, as given by the black circles plus solid line and red diamonds plus dashed line, respectively. (Right) Similar to the plot on the left, but for stellar mass, M_* , (black circles and solid line) and star-formation rate (red diamonds and dashed line). After removing the mean dependence of environment on color and luminosity, we find no significant residual trend with color, luminosity, stellar mass, or star-formation rate.

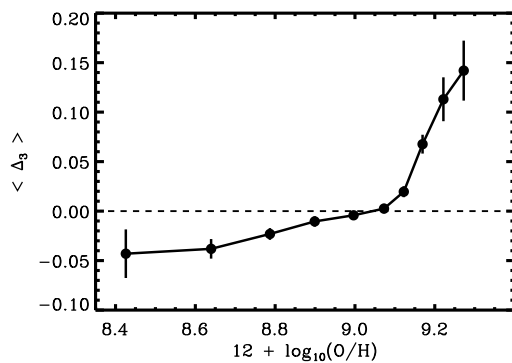


FIG. 8.— The dependence of mean residual environment, Δ_3 , on metallicity. We find a strong trend with metal-rich galaxies being found, on average, in regions of higher overdensity relative to galaxies of like color and luminosity.

est is the relationship between Low Ionization Nuclear Emission-line Regions (LINERs, Heckman 1980) and environment as low-level AGN such as LINERs are more likely to contaminate the star-forming sample than their more powerful Seyfert counterparts.

Using the SDSS data set, several studies of the relationship between AGN activity and environment have uncovered no significant correlation between low-level AGN activity and local galaxy density. For example, Miller et al. (2003) found that the fraction of AGN shows no variation with environment within the SDSS early data release (Stoughton et al. 2002), a result supported by later work using the larger DR4 data set (Sorrentino et al. 2006). While analysis by Montero-Dorta et al. (2008) shows that the fraction of LINERs and Seyferts on the red sequence is potentially lower in high-density environments locally, this result may not be representative of the environments of LINERs in the blue cloud (i.e., among the star-forming population). In partial agreement with the results of Montero-Dorta et al. (2008), Kauffmann et al. (2004) conclude that the fraction of galaxies hosting a powerful ($L[\text{O III}] > 10^7 L_\odot$) AGN

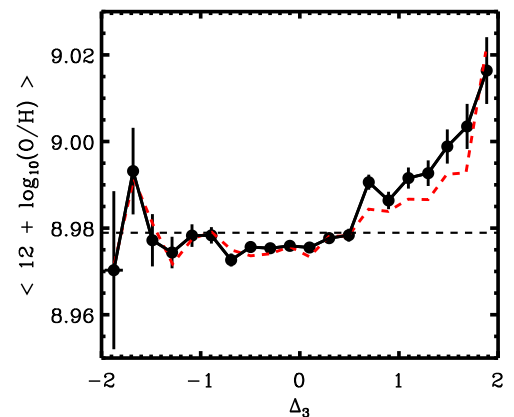


FIG. 9.— The dependence of mean (black points and solid line) and median (red dashed line) metallicity on the residual environment, Δ_3 . A strong correlation is found between residual environment and metallicity in overdense regions. This trend is evident, despite smearing effects related to the relatively large uncertainty in individual environment measures (see text) and the statistical dominance of galaxies with metallicities at $12 + \log_{10}(\text{O}/\text{H}) \sim 9$, where the metallicity-environment relation is weak (see Fig. 8). Note that in this figure the median relation has been offset by -0.03 in $12 + \log_{10}(\text{O}/\text{H})$ to facilitate display.

decreases in high-density environments. However, these are not the AGN that are likely to contaminate our star-forming sample. For low-level AGN activity, there is no evidence for a correlation with environment and thus it is unlikely that contamination from AGN would contribute to the observed correlation between metallicity and environment in our sample.

As shown by several studies of star-forming galaxies in the local Universe, there is a correlation between gas-phase oxygen abundance and galaxy morphology, such that more bulge-dominated systems are typically more metal-rich (e.g., Vila-Costas & Edmunds 1992; Zaritsky 1993; Zaritsky et al. 1994). An analogous trend is found when studying stellar metallicities among a more diverse galaxy population (Gallazzi et al. 2008). Any relation-

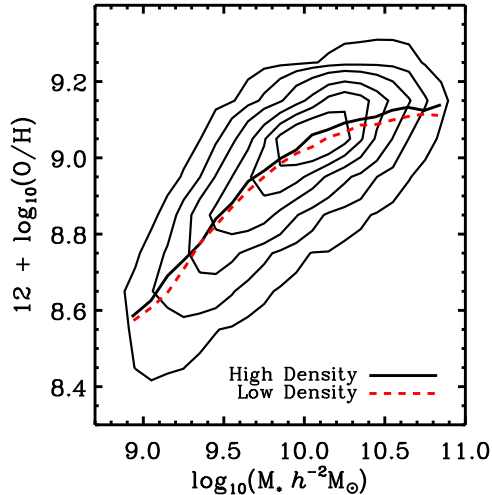


FIG. 10.— We plot the gas-phase oxygen abundance versus stellar mass for the star-forming sample and overplot the fits to the mass-metallicity relation in the extreme quintiles of the residual overdensity distribution. The contours correspond to galaxy numbers of $N_{\text{galaxy}} = 50, 200, 500, 1000, 1500, 2000$, while the solid black and dashed red lines show the median mass-metallicity relation for galaxies residing in high- and low-density regions, respectively. The lines follow the median metallicity values, computed in discrete bins of stellar mass. At all masses, the median metallicity of galaxies in high-density regions is greater than that of galaxies in low-density regions.

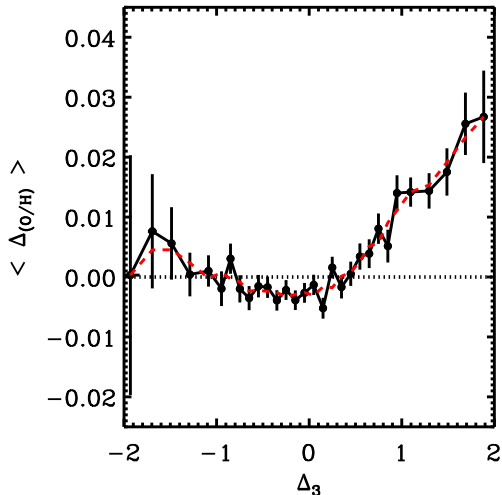


FIG. 11.— The median residual metallicity, relative to the median mass-metallicity relation, as a function of environment. We find a significant offset in metallicity (relative to the median mass-metallicity relation) as a function of galaxy overdensity. The dashed red line is the smoothed relation used to compute ϵ . Note that the dependence of the mean residual metallicity on environment closely follows the relation shown for the median residual metallicity.

ship between metallicity and environment separate from that observed with stellar mass could therefore be a derivative of the well-known morphology-density relation (e.g., Davis & Geller 1976; Dressler 1980).

Given the strong correlations between luminosity, color, and morphology on the blue cloud, the existence

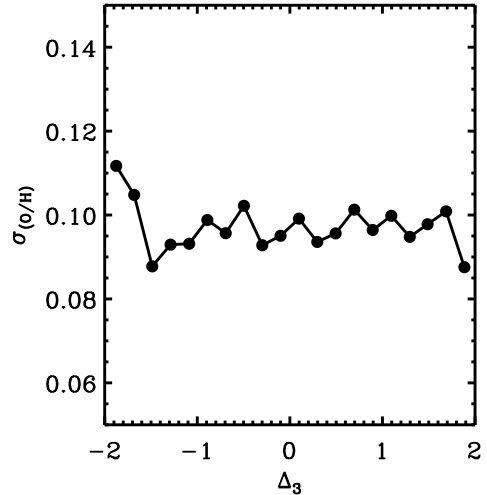


FIG. 12.— The root-mean-square of the deviations in the mass-metallicity relation as a function of environment. The intrinsic scatter (or “puffiness”) of the mass-metallicity relation shows no variation with environment. Note that the errors on $\sigma_{(\text{O}/\text{H})}$ are smaller than the data points, since each bin contains > 500 galaxies.

of a significant correlation between residual environment, Δ_3 , and morphology is unlikely when none is found with luminosity or rest-frame color. However, we investigate this possibility using the Sérsic indices of Blanton et al. (2003b, 2005a). While the Sérsic index is a measure of morphology derived from the fit of only a single component to the galaxy’s radial profile (versus bulge-disk decomposition, for example), we find no dependence of mean residual environment on Sérsic among our sample. Furthermore, recent analysis of star-forming galaxies in the SDSS found that the mass-metallicity relation shows no dependence on bulge fraction (Ellison et al. 2008a). Plus, as stated in §1, Tremonti et al. (2004) found no correlation between the scatter in the mass-metallicity relation and galaxy concentration. Thus, we conclude that the portion of the scatter in the mass-metallicity relation correlated with environment is not attributable to variations in galaxy morphology.

7.2. Theoretical Interpretation

As discussed in §1, gas-phase metallicity and its relationship with stellar mass within the star-forming population is directly connected to feedback associated with star formation, as metals are added to the ISM via supernovae and as gas is ejected via outflows and accreted from the surrounding intergalactic medium (IGM). The presence of outflows in star-forming galaxies has been supported by a variety of observations (e.g., Lehnert & Heckman 1996; Frye et al. 2002; Weiner et al. 2008), but the physics of this feedback mechanism remains poorly understood.

In an attempt to explain the mass-metallicity relation, early feedback models (e.g., Dekel & Silk 1986; Cole 1991; Dekel & Woo 2003) employed energy-driven winds, powered by supernovae explosions (Larson 1974), to expel metals from low-mass galaxies. Such models, however, fail to include the role of winds in more massive systems ($M_* \gtrsim 10^{10} M_\odot$), while observational work has shown outflows to be common at galaxy stellar masses of

$\gtrsim 10^{11} M_{\odot}$ (e.g., Shapley et al. 2003; Rupke et al. 2005; Weiner et al. 2008).

In contrast, the models of Springel & Hernquist (2003a) incorporate winds at all mass scales, but their simple prescription relies on winds of a constant velocity (484 km/s, Springel & Hernquist 2003b), independent of galaxy mass. In disagreement with this approach, recent observations by Martin (2005) show outflow velocities to scale approximately linearly with circular velocity (i.e., increase with M_*). Furthermore, simple wind approximations such as that of Springel & Hernquist (2003b) fail to reproduce some properties of the IGM at higher redshift (e.g., underpredicting metal enrichment, Aguirre et al. 2005) and the mass–metallicity relation at $z \sim 2$ (Finlator & Dave 2007).

Recent work by Finlator & Dave (2007) has ventured to take a more detailed approach to modeling the feedback in star-forming galaxies (see also Oppenheimer & Davé 2006). In their model, outflows are pushed by momentum-driven winds (Murray et al. 2005), where momentum is deposited into the ISM by coupling with the radiation from star formation through dust absorption and where the wind speed scales with the galaxy’s circular velocity. Rather than assuming a wind that is driven in all directions (such as that of Springel & Hernquist 2003a), Finlator & Dave (2007) model polar outflows with constrained opening angles ($\sim 45^\circ$) such that the resulting outflows much more closely imitate those observed locally (e.g., Veilleux et al. 2005).

In addition to assuming a wind speed that scales linearly with rotational speed, the Finlator & Dave (2007) model assumes that the mass-loading factor — the rate of mass ejection divided by the star-formation rate — is inversely related to the circular velocity. These scaling relations evolve naturally for momentum-driven winds (Murray et al. 2005) and are in rough agreement with results from other detailed feedback models (e.g., Kobayashi et al. 2007; Brooks et al. 2007). Within this theoretical framework, the gas-phase metallicity at any epoch depends on (i) the mean metallicity of accreted gas and (ii) the mass-loading factor (see Equation 20 of Finlator & Dave 2007).

In this model, the observed trends between metallicity and environment would require either higher enrichment of the gas flowing into galaxies in overdense regions and/or lower mass-loading factors in high-density environments. There are many environment-dependent physical mechanisms that could yield the former; for instance, supernova feedback from evolved stars associated with intragroup or intracluster light will directly dump metals (in particular, oxygen) into the IGM about galaxies in the highest-density environments. In addition, galaxy mergers, harassment, and ram-pressure stripping in groups and clusters can strip enriched gas from member and infalling galaxies, thereby inflating the metal content of the local gas reservoir relative to the gas supply of roughly primordial composition that feeds galaxies in the field (e.g., Gunn & Gott 1972; Moore et al. 1996; Hester 2006; Gnedin 1998).

Stripping of gas from cluster members could also contribute to a higher gas-phase metallicity in extreme environments in a secondary manner. That is, ram-pressure stripping could remove the outer portion (and therefore

most metal-poor segment) of a galaxy’s gas halo. Since the mixing time (assumed to be the dynamical time) for a disk galaxy is on the order of the cluster crossing time (~ 2 Gyr), if not stripped this metal-poor gas would become effectively mixed, thereby reducing the mean metallicity within the central $\sim 5 - 10$ kpc (the region sampled by an SDSS fiber).

In the most extreme environments, pressure from the intercluster medium (ICM) could potentially resist such stripping (e.g., Babul & Rees 1992). However, hydrodynamical simulations have found that the net effect of thermal pressure and ram-pressure stripping on a cluster member still results in gas being removed from the galaxy, contributing to the ICM (Murakami & Babul 1999). On the other hand, numerical and analytical modeling of feedback in isolated galaxies shows that the ejection of metals from a galaxy’s ISM is more likely to occur in regions of lower pressure (e.g., Silich & Tenorio-Tagle 2001; Mac Low & Ferrara 1999). Thus, thermal pressure (and its impact on the ability to drive an outflow) could account for the relative decrease in metallicity for galaxies in low-density environs.

Alternatively, the metallicity–environment relations presented in this work could also result from variations in the mass-loading factor with local galaxy density. While the mass-loading factor is, in principal, a quantity that can be directly observed (e.g., Morganti et al. 2005), detailed radio measurements of a galaxy’s gas mass are required. Since we lack the required observations within the SDSS data set, we instead utilize the SDSS spectroscopic data to look for signatures of variation in outflow velocity with environment at $z \sim 0.1$. Although, wind speed does not necessarily provide any information about the amount of mass expelled from a galaxy, a significant variation in outflow velocity with environment could be an indication that the net accretion rate (relative to the SFR) is driving the observed metallicity–environment relations. From co-adding two sets of spectra including several hundred strongly star-forming ($H\alpha$ equivalent width $> 30\text{\AA}$), massive ($M_* > 10^{10} M_{\odot}$) galaxies, we find no significant variation in the Na D absorption profile between extreme (low-density and high-density) environments. Admittedly, our analysis is limited to the most highly star-forming galaxies, given the low resolution ($R \sim 1800$) of the SDSS spectra.

Another point to consider when searching for physical sources of the strong relationship between environment and metallicity is that galaxies populating high-density regions today likely formed early in the first overdensities. Predictions of early galaxy enrichment (e.g., Schaye et al. 2003; Davé et al. 2006) indicate that these overdensities of gas at high- z would be the most enriched environments, naturally producing a metallicity–environment relation (see also Oppenheimer & Davé 2006). Within the model of Finlator & Dave (2007), however, the gas-phase metallicity in a galaxy at $z \sim 0.1$ is a product of the recent (< 1 Gyr) accretion and star-formation activity, rather than a result of the integrated star-formation history of the galaxy (see also Dalcanton 2007). So while galaxies in high-density environs in the local Universe generally formed early in cosmic time and in the early density peaks, metallicity–environment relations imprinted at $z \gtrsim 2$ would not necessarily persist to

the present.

7.3. Comparison to Related Work

As this paper was being completed, a parallel analysis of the relationship between metallicity and environment in the SDSS was presented by Mouhcine et al. (2007). Using a very similar data set, drawn from SDSS DR4 and employing the metallicity measurements of Tremonti et al. (2004), they find that the mass-metallicity relation depends weakly on local environment. When dividing our sample into discrete bins according to overdensity, we also find a relatively weak connection between metallicity and environment at fixed stellar mass (see Fig. 10); that is, when plotting the median mass-metallicity relation in discrete bins of overdensity, we find what appear to be only small variations among environment regimes, in close agreement with Figure 5 of Mouhcine et al. (2007).

However, studying the relationships between galaxy properties and environment in this manner is far less sensitive than the techniques presented herein. Measurements of local galaxy density are inherently noisier than measures of other galaxy properties, including rest-frame color, luminosity, stellar mass, and metallicity. Thus, when dividing a sample by environment, any trends in the data set are smeared out by the significant correlation between neighboring bins. While Mouhcine et al. (2007) conclude that gas-phase oxygen abundance is only weakly dependent on environment, we have presented evidence to the contrary, showing that the metallicity-environment relation is roughly equal in strength to the color-density relation. Furthermore, we find metallicity has a relationship with environment that is separate from the color-density or stellar mass-density relations.

In contrast to our work and that of Mouhcine et al. (2007), which trace galaxy environments on $\sim 1-2h^{-1}$ Mpc scales over the full SDSS galaxy population, the analyses of Kewley et al. (2006) and Ellison et al. (2008b) probe a far more limited range of environments, focusing on the metallicity of galaxy pairs in the local Universe. Focusing on smaller scales, they find that galaxy pairs at close (projected) separations ($\lesssim 30 h^{-1}$ kpc) are biased towards lower metallicities. This result is attributed to inflows of metal-poor gas during the merger or interaction process, an effect that is also found in simulations (Perez et al. 2006). The number of close (projected separations $< 100 h^{-1}$ kpc) pairs, however, is $\lesssim 1\%$ in the SDSS sample (see also Deng et al. 2006), and thus such systems cannot be a significant contribution to the scatter in the mass-metallicity relation. While metallicity may be lower in close pairs, the dominant metallicity-environment relation moves towards higher metal enrichment in high-density environments.

8. SUMMARY AND CONCLUSIONS

Using the measurements of gas-phase oxygen abundance from Tremonti et al. (2004) and local galaxy environment from Cooper et al. (2008), we study the relationship between metallicity and environment in a sample of star-forming galaxies drawn from the SDSS data set. Our principal results are as follows.

1. We find a strong metallicity-density relation (see Fig. 3b) in the local Universe such that more

metal-rich galaxies favor regions of higher galaxy overdensity. This relationship between metallicity and environment follows (with comparable or greater strength) that seen between environment and other fundamental properties such as color, luminosity, SFR, or stellar mass.

2. After removing the mean color-luminosity-environment relation from the SDSS data set, we find a significant residual relationship between environment and metallicity (see Fig. 8), suggesting that metallicity has a relationship with environment separate from that observed with color and luminosity (or with stellar mass).
3. The residual metallicity-environment trend is largely driven by galaxies in high-density regions such as groups and clusters, where the local environment may be responsible for impacting the feedback and/or gas accretion relative to galaxies of like stellar mass in lower-density regions.
4. A non-negligible portion (at least 15%) of the scatter in the mass-metallicity relation is correlated with local environment.

Support for this work was provided by NASA through the Spitzer Space Telescope Fellowship Program. C.A.T. acknowledges support by NASA through Hubble Fellowship grant HST-HF-01192.01, awarded by the Space Telescope Science Institute, which is operated by AURA Inc. under NASA contract NAS 5-26555. M.C.C. would like to thank Michael Blanton, David Hogg, and Renbin Yan for their assistance in utilizing the NYU-VAGC data products. This work benefited greatly from conversations with Kristian Finlator, Romeel Davé, Ben Weiner, and Dennis Zaritsky.

Funding for the SDSS has been provided by the Alfred P. Sloan Foundation, the Participating Institutions, the National Science Foundation, the U.S. Department of Energy, the National Aeronautics and Space Administration, the Japanese Monbukagakusho, the Max Planck Society, and the Higher Education Funding Council for England. The SDSS Web Site is <http://www.sdss.org/>.

The SDSS is managed by the Astrophysical Research Consortium for the Participating Institutions. The Participating Institutions are the American Museum of Natural History, Astrophysical Institute Potsdam, University of Basel, University of Cambridge, Case Western Reserve University, University of Chicago, Drexel University, Fermilab, the Institute for Advanced Study, the Japan Participation Group, Johns Hopkins University, the Joint Institute for Nuclear Astrophysics, the Kavli Institute for Particle Astrophysics and Cosmology, the Korean Scientist Group, the Chinese Academy of Sciences (LAMOST), Los Alamos National Laboratory, the Max-Planck-Institute for Astronomy (MPIA), the Max-Planck-Institute for Astrophysics (MPA), New Mexico State University, Ohio State University, University of Pittsburgh, University of Portsmouth, Princeton University, the United States Naval Observatory, and the University of Washington.

REFERENCES

- Adelberger, K. L., Shapley, A. E., Steidel, C. C., Pettini, M., Erb, D. K., & Reddy, N. A. 2005, *ApJ*, 629, 636
- Adelman-McCarthy, J. K. et al. 2006, *ApJS*, 162, 38
- Aguirre, A., Schaye, J., Hernquist, L., Kay, S., Springel, V., & Theuns, T. 2005, *ApJ*, 620, L13
- Babul, A. & Rees, M. J. 1992, *MNRAS*, 255, 346
- Balogh, M. et al. 2004a, *MNRAS*, 348, 1355
- Balogh, M. L., Baldry, I. K., Nichol, R., Miller, C., Bower, R., & Glazebrook, K. 2004b, *ApJ*, 615, L101
- Balogh, M. L., Schade, D., Morris, S. L., Yee, H. K. C., Carlberg, R. G., & Ellingson, E. 1998, *ApJ*, 504, L75+
- Blanton, M. R., Eisenstein, D., Hogg, D. W., Schlegel, D. J., & Brinkmann, J. 2005a, *ApJ*, 629, 143
- Blanton, M. R. & Roweis, S. 2007, *AJ*, 133, 734
- Blanton, M. R. et al. 2003a, *AJ*, 125, 2348
- . 2003b, *ApJ*, 594, 186
- . 2005b, *AJ*, 129, 2562
- Brinchmann, J., Charlot, S., White, S. D. M., Tremonti, C., Kauffmann, G., Heckman, T., & Brinkmann, J. 2004, *MNRAS*, 351, 1151
- Brodie, J. P. & Huchra, J. P. 1991, *ApJ*, 379, 157
- Brooks, A. M., Governato, F., Booth, C. M., Willman, B., Gardner, J. P., Wadsley, J., Stinson, G., & Quinn, T. 2007, *ApJ*, 655, L17
- Bruzual, G. & Charlot, S. 2003, *MNRAS*, 344, 1000
- Capak, P., Abraham, R. G., Ellis, R. S., Mobasher, B., Scoville, N., Sheth, K., & Koekemoer, A. 2007, *ApJS*, 172, 284
- Cavaliere, A., Colafrancesco, S., & Menci, N. 1992, *ApJ*, 392, 41
- Chabrier, G. 2003, *PASP*, 115, 763
- Charlot, S. & Longhetti, M. 2001, *MNRAS*, 323, 887
- Cole, S. 1991, *ApJ*, 367, 45
- Contini, T., Treyer, M. A., Sullivan, M., & Ellis, R. S. 2002, *MNRAS*, 330, 75
- Cooper, M. C., Newman, J. A., Madgwick, D. S., Gerke, B. F., Yan, R., & Davis, M. 2005, *ApJ*, 634, 833
- Cooper, M. C. et al. 2006, *MNRAS*, 370, 198
- . 2007, *MNRAS*, 376, 1445
- . 2008, *MNRAS*, 383, 1058
- Cucciati, O. et al. 2006, *A&A*, 458, 39
- Dalcanton, J. J. 2007, *ApJ*, 658, 941
- Davé, R., Finlator, K., & Oppenheimer, B. D. 2006, *MNRAS*, 370, 273
- Davis, M. & Geller, M. J. 1976, *ApJ*, 208, 13
- Dekel, A. & Silk, J. 1986, *ApJ*, 303, 39
- Dekel, A. & Woo, J. 2003, *MNRAS*, 344, 1131
- Deng, X.-F., Chen, Y.-Q., Wu, P., Luo, C.-H., & He, J.-Z. 2006, *Chinese Journal of Astronomy and Astrophysics*, 6, 411
- Domainko, W., Gitti, M., Schindler, S., & Kapferer, W. 2004, *A&A*, 425, L21
- Dressler, A. 1980, *ApJ*, 236, 351
- Ellison, S. L., Patton, D. R., Simard, L., & McConnachie, A. W. 2008a, *ApJ*, 672, L107
- . 2008b, *ApJ*, *ApJ*, accepted
- Erb, D. K., Shapley, A. E., Pettini, M., Steidel, C. C., Reddy, N. A., & Adelberger, K. L. 2006, *ApJ*, 644, 813
- Finlator, K. & Dave, R. 2007, *ArXiv e-prints*, 704
- Frye, B., Broadhurst, T., & Benítez, N. 2002, *ApJ*, 568, 558
- Gallazzi, A., Brinchmann, J., Charlot, S., & White, S. D. M. 2008, *MNRAS*, 383, 1439
- Garnett, D. R. 2002, *ApJ*, 581, 1019
- Gnedin, N. Y. 1998, *MNRAS*, 294, 407
- Gunn, J. E. & Gott, J. R. I. 1972, *ApJ*, 176, 1
- Heckman, T. M. 1980, *A&A*, 87, 152
- Hester, J. A. 2006, *ApJ*, 647, 910
- Hogg, D. W. et al. 2003, *ApJ*, 585, L5
- Kauffmann, G., White, S. D. M., Heckman, T. M., Ménard, B., Brinchmann, J., Charlot, S., Tremonti, C., & Brinkmann, J. 2004, *MNRAS*, 353, 713
- Kauffmann, G. et al. 2003a, *MNRAS*, 341, 33
- . 2003b, *MNRAS*, 346, 1055
- Kewley, L. J., Geller, M. J., & Barton, E. J. 2006, *AJ*, 131, 2004
- Kobayashi, C., Springel, V., & White, S. D. M. 2007, *MNRAS*, 376, 1465
- Kobulnicky, H. A. et al. 2003, *ApJ*, 599, 1006
- Lamareille, F., Mouhcine, M., Contini, T., Lewis, I., & Maddox, S. 2004, *MNRAS*, 350, 396
- Larson, R. B. 1974, *MNRAS*, 169, 229
- Lee, H., McCall, M. L., & Richer, M. G. 2003, *AJ*, 125, 2975
- Lee, H., Skillman, E. D., Cannon, J. M., Jackson, D. C., Gehrz, R. D., Polomski, E. F., & Woodward, C. E. 2006, *ApJ*, 647, 970
- Lehnert, M. D. & Heckman, T. M. 1996, *ApJ*, 472, 546
- Lequeux, J., Peimbert, M., Rayo, J. F., Serrano, A., & Torres-Peimbert, S. 1979, *A&A*, 80, 155
- Mac Low, M.-M. & Ferrara, A. 1999, *ApJ*, 513, 142
- Martin, C. L. 2005, *ApJ*, 621, 227
- Miller, C. J., Nichol, R. C., Gómez, P. L., Hopkins, A. M., & Bernardi, M. 2003, *ApJ*, 597, 142
- Montero-Dorta, A. D. et al. 2008, *ArXiv e-prints*, 801
- Moore, B., Katz, N., Lake, G., Dressler, A., & Oemler, A. 1996, *Nature*, 379, 613
- Morganti, R., Tadhunter, C. N., & Oosterloo, T. A. 2005, *A&A*, 444, L9
- Mouhcine, M., Baldry, I. K., & Bamford, S. P. 2007, *MNRAS*, 382, 801
- Murakami, I. & Babul, A. 1999, *MNRAS*, 309, 161
- Murray, N., Quataert, E., & Thompson, T. A. 2005, *ApJ*, 618, 569
- Oke, J. B. & Gunn, J. E. 1983, *ApJ*, 266, 713
- Oppenheimer, B. D. & Davé, R. 2006, *MNRAS*, 373, 1265
- Peeples, M. S., Pogge, R. W., & Stanek, K. Z. 2008, *ArXiv e-prints*, 804
- Perez, M. J., Tissera, P. B., Scannapieco, C., Lambas, D. G., & de Rossi, M. E. 2006, *A&A*, 459, 361
- Pilyugin, L. S. & Ferrini, F. 2000, *A&A*, 354, 874
- Rupke, D. S., Veilleux, S., & Sanders, D. B. 2005, *ApJS*, 160, 115
- Salim, S. et al. 2007, *ApJS*, 173, 267
- Schaye, J., Aguirre, A., Kim, T.-S., Theuns, T., Rauch, M., & Sargent, W. L. W. 2003, *ApJ*, 596, 768
- Shapley, A. E., Coil, A. L., Ma, C.-P., & Bundy, K. 2005, *ApJ*, 635, 1006
- Shapley, A. E., Steidel, C. C., Pettini, M., & Adelberger, K. L. 2003, *ApJ*, 588, 65
- Silich, S. & Tenorio-Tagle, G. 2001, *ApJ*, 552, 91
- Skillman, E. D., Kennicutt, R. C., & Hodge, P. W. 1989, *ApJ*, 347, 875
- Smith, G. P., Treu, T., Ellis, R. S., Moran, S. M., & Dressler, A. 2005, *ApJ*, 620, 78
- Sorrentino, G., Radovich, M., & Rifatto, A. 2006, *A&A*, 451, 809
- Springel, V. & Hernquist, L. 2003a, *MNRAS*, 339, 289
- . 2003b, *MNRAS*, 339, 312
- Stoughton, C. et al. 2002, *AJ*, 123, 485
- Tremonti, C. A. et al. 2004, *ApJ*, 613, 898
- Veilleux, S., Cecil, G., & Bland-Hawthorn, J. 2005, *ARA&A*, 43, 769
- Vila-Costas, M. B. & Edmunds, M. G. 1992, *MNRAS*, 259, 121
- Weiner, B. J. et al. 2008, *ApJ*, in prep
- York, D. G. et al. 2000, *AJ*, 120, 1579
- Zaritsky, D. 1993, *PASP*, 105, 1006
- Zaritsky, D., Kennicutt, Jr., R. C., & Huchra, J. P. 1994, *ApJ*, 420, 87